iPSRS

ERASMUS MUNDUS JOINT MASTER

Intelligent Photonics for Security Reliability Sustainability & Safety

Master *Intelligent Photonics for Security Reliability Sustainability and Safety* (iPSRS)

Université Jean Monnet Saint-Étienne

UNIVERSITY OF EASTERN FINLAND

UPEC UNIVERSITÉ PARIS-EST CRÉTEIL VAL DE MARNE

VILNIAUS UNIVERSITETAS · 1579 · UNIVERSITAS VILNENSIS

LASER ENGRAVING ON STAINLESS-STEEL AND MAPLE WOOD AS A MEANS OF CUSTOMIZING PAYMENT CARDS

Internship Report

Presented by

Teagan Kilian

and defended at

University Jean Monnet

September 4th, 2025

Academic Supervisor: University Professor, Dr. Matthieu Roussey, University of Eastern Finland

Host Supervisor: R&D Project Manager, Jessica Pellegrino, Toppan Security

Jury Committee: University Professor & iPSRS Coordinator, Dr. Nathalie Destouches, Université Jean Monnet

University Professor, Dr. Amine Naït-Ali, Université Paris-Est Créteil

University Professor, Dr. Victor Kalt, Université Jean Monnet

University Professor, Dr. Thibault Girardin, Université Jean Monnet

Abstract

As part of an internship assignment given by *Toppan Security*, a set of tests were designed to evaluate the engraving effect of various laser parameters - laser speed, laser power, hatch (line density), and pulse frequency - on both maple wood and stainless-steel samples. A CO_2 laser, two blue diode lasers, and an infrared fiber laser, all from the company *xTool Laser*, were used in this study. These tests were designed to examine parameters that would be valuable in the case of using laser engraving as a method for customizing payment cards made primarily out of these non-traditional materials.

Toppan Security is a subsidiary of *Toppan* - a Japan-based company - which was historically active in the printing industry. Currently, *Toppan Security* has major global roles in security and more precisely, the payment and identity sectors. They are interested in widening the range of products offered to their payment card clients in order to remain a competitive player in the industry.

The current market has hybrid payment cards made of both metal and polyvinyl chloride [PVC] available with some all-metal cards also available. Today, *Toppan Security* provides payment cards with a metal core (PVC on either side), but they are interested in providing a more high-end and exclusive customer experience by offering a payment card which is less reliant on plastic. Wooden payment cards are also currently available to customers as a more environmentally friendly alternative to the typical plastic payment card.

The tests included a writing test, a resolution test, a minimum line thickness test, and a color test (only on the metal samples). These tests were designed to examine parameters that would be valuable in the case of using laser engraving as a method for customizing payment cards.

The outcomes of the writing, resolution and line trials revealed that the three lasers (CO_2 and both blue lasers) used on wood were all well equipped for laser engraving on this material.

The stainless-steel trials suggested that for a wide range of parameters in different combinations, fiber laser engraving on stainless steel will allow for full-metal payment cards with great customization potential. This laser can even be used for laser marking to add colors to the product if adequate cooling and air circulation is added to the machines.

Table of Contents

Laser Engraving on Stainless-Steel and Maple Wood
as a Means of Customizing Payment Cards

Teagan Kilian

1. Introduction

In relation to *Toppan Security's* research and development efforts regarding payment card advances, a series of laser engraving trials were carried out on two different materials: maple wood and stainless steel.

Wooden payment cards provide a more sustainable alternative to the typical plastic card. The question is whether these cards can be customized using laser engraving techniques.

Metal payment cards are not new; however, the current market includes hybrid cards which are some combination of polyvinyl chloride [PVC] and metal layers. The PVC allows more freedom and ease when it comes to customizing the cards. *Toppan's* goal is to create a payment card that can have a metal face or be made entirely out of metal. This would give the user a sense of luxury due to the weight of the cards and the sound that it makes when it is dropped. These cards would be reserved for high status customers in order to preserve the allure of their exclusivity. This type of product is already being introduced to the market by some of *Toppan Security's* competitors.

If this goal is to be achieved, there needs to be a repeatable and reliable method of customizing directly on the metal surface. Several processes can be applied to decorate metal like chemical treatment, thermal oxidation, direct printing, and laser processing. The focus during the internship will be to explore laser marking on metal.

Laser engraving on stainless steel using infrared lasers is already a well understood topic. Laser marking; however, is still prevalent in research. These methods can produce color changes to the surface of the metal and the color that is produced is generally dependent on the temperature which the laser heats the medium to and on the materials absorption. Ultimately it is the laser parameters which provide these effects, and they should be tuned accordingly [1].

As part of a collaboration between *Toppan Security* and *Université Jean Monnet*, these tests were completed inside of the University's student laser platform.

The aim of these trials was to understand how an infrared laser can interact with the material and how the laser parameters can be leveraged to produce different effects on the stainless steel or wood surfaces. With this knowledge, a method will be defined for parameter optimization in order to produce a laser engraved, alternative material payment cards which have all text and designs clearly visible.

2. State of the Art

2.1. Laser Irradiation of Wood

Using lasers to engrave on wood – specifically CO_2 or blue lasers – is a well-studied subject. Due to the organic and non-uniform nature of wood, it is important to remember that even if parameters and their effects are well understood, it would be hard to exactly predict how the material will react.

2.1.1. Engraving Mechanism

According to Kúdela et al. (in their study observing the effects of a CO_2 laser on spruce wood), the changes observed on wood post laser processing occur both due physical (structural) and chemical changes to the surface of the material [2].

On the chemical side, the heat produced by the laser causes bonds within chromophore structures to break. Chromophore is found within the lignin and hemicellulose structures of wood and gives wood its color. Evidently, the breaking of bonds within the chromophore is what causes the change of color when wood is exposed to high enough temperatures. In a different study by Kúdela et al. focusing on oak wood, it was found that the number of polysaccharides present in the wood post processing was inversely proportional to the energy of the laser beam [3]. The exact chemical reactions resulting from laser irradiation on wood depend on the individual species of wood due to their unique chemical composition [2].

Namely, the temperature at which visible charring occurs on wood is the pyrolysis temperature. Pyrolysis is the first step in the combustion process; it occurs without oxygen and generally at a temperature between 400° C and 900° C [4]. When this temperature is reached (in this case through contact with a laser beam) the color change occurs in the shape of a gaussian profile. The color change will be the most intense at the center of the laser spot and it will gradually fade out [5].

Physically, one result of laser irradiation on wood is the sublimation of a portion of the wood surface followed by melting and a carbonized layer forming. Effectively, the wood sample will experience a loss of mass and a newly introduced surface roughness [2]. Increased laser hatch led to more material being removed and therefore a greater loss of mass. Interestingly, lower levels of irradiation can have a smoothing effect on the wood until the irradiation is high enough to cause the carbonization layer to form. This was observed by Kúdela et al. in their oak wood study [3].

2.1.2. Possible Colors

Evidently, there are adjustable laser parameters which can be utilized to intentionally produce darker or lighter engravings. Increasing the power and hatch of the laser led to a more dramatic color change on the wood [3]. According to the engraving tests on birch wood using a blue laser carried out by Chernykh et al., the color of the irradiated wood, more specifically the hue, is specific to wood species. Even so, using this method of surface modification, it is not possible to obtain a hue value of 100% for any wood species (a hue value of 100% correlates to the surface being visibly black) [5].

The wood material used in these trials was maple wood. Although the specific reaction due to laser-wood interactions are specific to the wood species, the general trends are expected to be the same.

2.2. Laser Irradiation of Stainless Steel

Laser processing of metal has been used in many industries for years. The typical roles of lasers in industry are cutting or engraving which are very favorable manufacturing methods due to fast processing times, and a very concentrated and easily controllable source of heat [6]. More traditional mechanical manufacturing processes have moving parts which come in contact with the materials being processed which leads to parts wearing down and needing to be replaced over time. This is not the case with lasers because there is no direct contact between the machinery and the material.

Widely used methods of non-laser color marking on metal include printing, emulsion coating or electrolytic oxidation. These methods have many drawbacks including complex processing and color instability due to time or wear. According to Antonczak et al., laser color marking has greatly piqued the interest of a variety of industries; however, major challenges remain, chiefly lack of repeatability [7].

2.2.1. Laser Engraving

Due to the high precision and control associated with laser engravings, it is among the most used laser processes. Important parameters to consider in terms of laser engraving include the power density and wavelength of the laser used. Nikolidakis et al. claims that a minimum power density of 10^8 W/cm^2 must be used to remove material from the surface of a stainless-steel sample. Additionally, the reflectivity of reflective surfaces is dependent on the wavelength of the incident light, the type of laser must be chosen with the specific material in mind. One should choose a laser in the wavelength which the metal experiences low reflectivity [8].

In general, laser ablation is the mechanism which engraves the metal sample. Assuming that the laser is pulsed, each pulse removes a certain area with a certain depth from the material's surface. Consecutive pulses will overlap which allows for a consistent depth throughout the engraved surface [8].

2.2.2. Laser Color Marking

Colors can be produced on metal using laser processing in two ways: surface oxidation and laser induced periodic surface structures (LIPSS). This report will focus on surface oxidation as a means to produce color.

The highly concentrated and intense heat of the laser on the metal causes the production of an oxide surface layer. In contrast to the behavior of a typical metal surface – where the internal particles absorb most photons of incident white light and the surface particles reflect it – the white light interacts with the oxide in a different way. As white light approaches the metal, some light is initially reflected while some is absorbed into the oxide layer, refracted, then reflected at the interface of the metal and the oxide [6]. The layer causes interference between rays of light which enter through the oxide layer and those which have entered the oxide layer and are reflected by the metallic surface beneath [7]. Figure 1 depicts the interaction of the light and material which produces color. The oxide layer also provides an anti-corrosion coating to the metal which proves to be favorable in terms of product longevity [9].
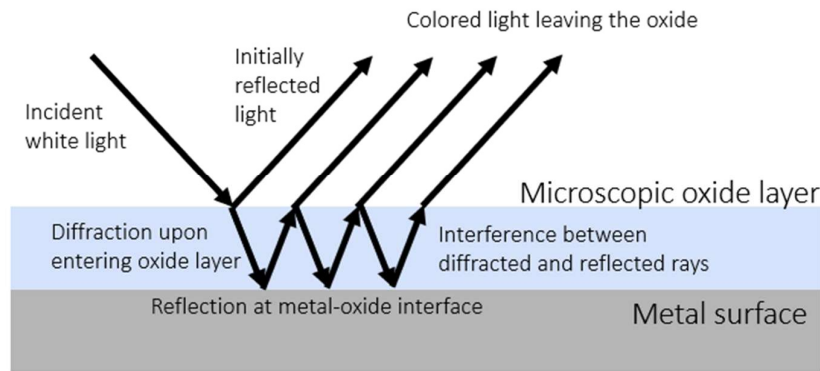

Figure 1: Production of colored light from white light due to an oxidation film on a metal surface

Veiko et al. propose a metric base on temperature and time which can aid in color prediction, known as the technical chromaticity coefficient:

$$C_{tech} = T(Nx) \cdot t_{eff_{xy}} .$$
(1)

The value of $T(N_x)$ represents the maximum temperature reached by the surface of the material in the x-direction. This is dependent on the number of pulses in the same direction (N_x). $T(N_x)$ can be calculated by the following formula:

$$T(N_x) = \frac{2I(1-R)\sqrt{a}}{k\sqrt{\pi}} \cdot \sum_{n=0}^{N_x} \left[\sqrt{t(N_x) - \frac{n}{f}} - \sqrt{t(N_x) - \left(\frac{n}{f} + \tau\right)} \right] + T_0 \quad \textbf{(2)}$$

where

$$t(N_x) = \frac{N_x}{f} + \tau, \quad \textbf{(3)}$$

R is the reflectivity of the material at the laser's wavelength, a is the thermal diffusivity, k is the thermal conductivity, τ is the pulse duration, and f is the laser's frequency.

The second parameter for which C_{tech} depends on is the effective time of action per unit surface area. The following formula can be used to calculate this value:

$$t_{eff\_xy} = N_x N_y \tau = (1 - L_x)(1 - L_y) \cdot \tau, \quad \textbf{(4)}$$

where L_x and L_y are the pulse overlaps in their respective directions [9]. These values can be calculated by the following formula according to Nikolidakis et al.:

$$L_x = 1 - \frac{v}{f d_o}, \quad \textbf{(5)}$$

where v is the velocity of the laser and d_o is the laser spot diameter [8].

In the study carried out by Veiko et al., it was found that the color associated with the C_{tech} value was unique to the specific type of metal. Each metal can produce a similar color within a range of effective time of action and maximum temperature values but, these colors are unique to the metal species [9].

Figure 2 reveals how one can predict color based on the technical chromaticity coefficient, according to Veiko et al. [9].
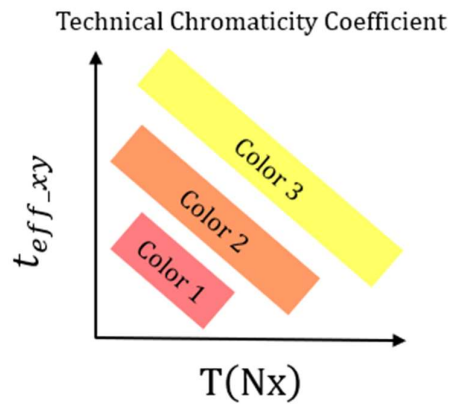

Figure 2: Plot depicting the relationship between the technical chromaticity coefficient and color

Facilitating oxide growth is very important to the visibility of colors on metal surfaces. As an overview, this process includes heating the material to a temperature where the air, specifically the oxygen, begins to react with the metal surface. First, the oxygen is absorbed by the metal surface followed by the generation of ionic bonds between the molecules in the oxygen and the metal. This reaction grows laterally - so it ends up being continuous throughout the irradiated surface – then, vertically due to diffusion of ions at the interface of the oxide and the metal. The vertical growth of the oxide layer is related to the amount of energy absorbed from the laser. Ultimately, it is the difference in oxide thickness which produces the appearance of distinct colors [6].

3. Experimental Approach

3.1. Materials

The samples used in these tests were purchased and provided by *Toppan* Security. All laboratory equipment was provided by either *Toppan*, *Laboratory Hubert Curien*, or the student laser platform of *University Jean Monnet.*

3.1.1. Samples

Considering that the aim of this internship was to explore alternative materials which could be used as payment cards. The two materials of interest for these tests are wood and metal. The wood tests were carried out on thin card-sized samples of maple wood. The exact dimensions were as follows: 85.70 x 53.95 x 0.87 mm.

Two different types of stainless-steel alloy 301 samples were used in the metal trials. The first were square sheets with the exact dimensions being 101.90 x 101.90 x 0.47 mm. The second type of sample was a hybrid metal and PVC cards with the dimensions of 85.55 x 53.93 x 0.83 mm. The hybrid card included a layer of stainless steel on one side of the card and a layer of PVC on the card's reverse side. The thickness of the metal layer is 0.47 mm.

All stainless-steel samples were placed in an ultrasonic bath with demineralized water for five minutes post-processing to remove any debris or dust that could have accumulated.

3.1.2. Lasers

Five different laser engravers - four of them produced by the company *xTool Laser* - were used to mark the wood cards. The parameters of each laser used in these trials are seen in table 1. The first model is their *P2S* CO_2 laser. This laser has a maximum output power of 55 W. The wavelength of this laser is within the far infrared range, specifically, at 10.6 µm [10].

Laser Manufacturer	xTool				Otto Kuennecke
Model	PS2	S1	F1 Ultra		DPS smart
Power (W)	55	40	20	20	20
Wavelength (µm)	10.6	0.455	0.455	1.064	1.064
Beam size (mm)	0.15 x 0.15	0.08 x 0.1	0.08 x 0.1	0.03 x 0.03	

Table 1: Parameters of each laser used in these trials [10]

The second laser is the *S1* model. This blue-diode laser has a maximum output power of 40 W and a wavelength of 455 nm [10].

The last laser is an *xTool F1 Ultra* model. This laser has the capability to produce both a blue diode and an infrared fiber laser beam with an output power of 20 W. The blue laser has a wavelength of 455 nm, and the infrared laser has a wavelength of 1064 nm ± 5 nm [10].

The spot size of each of the laser beams was provided on the *xTool Laser* website and they are shown in table 1 as well. In the case of the *F1 Ultra* infrared laser, this value is considered to be the laser waist for calculations throughout the report.

Finally, a second infrared laser - *Otto Kuennecke DPS smart* - was used. This laser is specifically designed for laser marking on polycarbonate passports and ID cards [11]. This laser is a YAG fiber diode pump laser and also has a wavelength of 1064 nm and an output power of 20 W. The pulse repetition rate used with this laser was 100 kHz.

3.1.3. Software

The software *xTool Creative Space* was used in conjunction with the lasers to define their parameters and engraving patterns. The software has three modes: scoring, engraving, and cutting. The scoring mode is used to process the outline of a shape without cutting entirely through the material. The engraving mode fills in the area of the specified shape. This mode was used exclusively for all tests with all lasers. Finally, the cutting mode is used to produce through cuts in a material [12].

Python, Microsoft Office Excel, and *Image J* were valuable tools used in processing the data obtained in these trails.

3.1.4. Characterization equipment

A portable *eXact* reflectance spectrophotometer from the manufacturer *X-Rite Pantone* was used to extract color data from the stainless-steel surface produced by laser processing. This spectrophotometer describes the colors based on the CIE L*a*b* color space. This device measures from an angle of 45°. The measurements taken for these trials used the M1 setting which included CIE standard illuminant D50 which has a color temperature of 5000K [13]. Illuminant D50 is the standard illuminant used in the printing industry. The accuracy of these measurements had to be considered due to the reflectivity of the stainless-steel surface.

In order to observe the fine details of the engravings, a *Nikon SMZ1270* zoom stereo microscope was used along with the *Plan Apo* 0.5x/WF objective [14]. The microscope was also equipped with a *μEye* camera to take the images.

3.2. Experimental conditions

The laser parameters of interest in these tests include the speed, power, hatch (number of lines engraved per centimeter), and pulse frequency (in the case of the *F1 Ultra* infrared laser). The limits of each of these parameters - as per the abilities of each laser - are seen in table 2Table .

	P2S	S1	F1 Ultra
Speed (mm/s)	0 − 600	0 − 600	0 − 10,000
Power (%)	0 − 100	0 − 100	0 − 100
Power (W)	0 − 55	0 − 40	0 − 20
Hatch (L/cm)	0 − 300	0 − 300	0 − 300
Frequency (kHz)	NA	NA	30 − 60

Table 2: Laser parameter limits for each laser

Additionally, the distance between the laser and the engraving surface could be changed manually; however, the auto-focus function was used to find the focal length for all tests. The distance between the surface of the sample and the laser head was stated in *xTool Creative Space* before each laser run. The average value for each laser is noted in table 3Table 3.

Model	Laser head - sample distance (mm)
P2S	1.36
F1 Ultra	16.28
S1	22.51

Table 3: Average distance between laser head and sample using the auto-focus feature

Since each laser had a different output power, in order to compare results accurately, the power percentages were converted to their corresponding power in watts. As seen in table 4Table 4, the conversion was used to compare results produced with the same nominal output power.

Some of the tested output powers do not have an exact match from laser to laser; however, among these powers, the average difference is only 2.4%. Their differences are sufficient to compare the capabilities of the three laser models.

PS2 Power	PS2 Watts	S1 Power	S1 Watts	F1 Ultra Power	F1 Ultra Watts
				10.00%	2
				15.00%	3
		10.00%	4	20.00%	4
10.00%	5.5			25.00%	5
		15.00%	6	30.00%	6
				35.00%	7
15.00%	8.25	20.00%	8	40.00%	8
				45.00%	9
		25.00%	10	50.00%	10
20.00%	11			55.00%	11
		30.00%	12	60.00%	12
25.00%	13.8	35.00%	14	70.00%	14
30.00%	16.5	40.00%	16	80.00%	16
		45.00%	18	90.00%	18
35.00%	19.3	50.00%	20	100.00%	20
40.00%	22	55.00%	22		
45.00%	24.8	60.00%	24		
50.00%	27.5	70.00%	28		
55.00%	30.3	80.00%	32		
60.00%	33	90.00%	36		
70.00%	38.5	100.00%	40		
80.00%	44				
90.00%	49.5				
100.00%	55				

Table 4: Aid for a more accurate comparison of laser parameters between the different laser models

3.3. Tests

There were three main categories of tests in general: resolution, line thickness, and writing. These tests were done on the wood samples using the *P2S, S1,* and *F1 Ultra* blue lasers. The resolution and writing tests were also completed using the *F1 Ultra* infrared laser on the metal samples. Depending on the material (metal or wood), additional tests were performed. The additional tests done on wood were performed with the *Otto Kuenneke* infrared laser. The additional tests done on the metal samples were the color tests to explore laser marking on stainless steel.

3.3.1. Resolution Tests

During the resolution tests, patterns with alternating lines and spaces of the same distance were engraved at different orientations. These line patterns were drawn vertically, horizontally, and at a 45° angle (relative to the placement of the sample within the laser enclosure). This design was repeated for line and space thicknesses of 0.5, 0.4, 0.3, 0.2, 0.1, 0.08, 0.05, and 0.03 mm. These tests were repeated at a variety of speeds and output powers as seen in figure 3Figure 3. The aim of this test was to define the parameters that produce the best resolution.
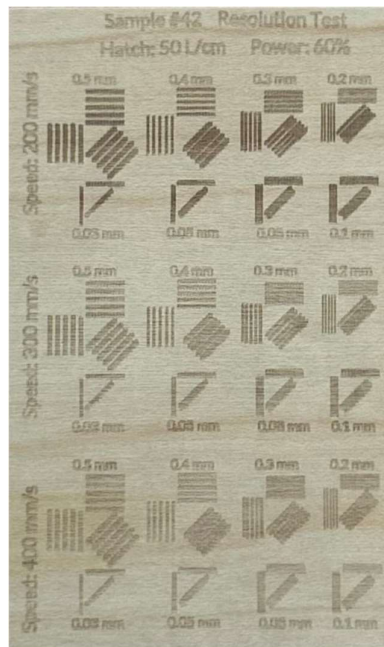

Figure 3: Example of resolution test done with the P2S *laser on a wooden sample*

3.3.2. Writing Tests

The purpose of the writing tests were to observe the resolution and readability of various fonts and font sizes. To ensure uniform testing, the word *Toppan* was used as the test word for all of these tests. Variables that were changed during the writing tests were font, power, speed, hatch, and pulse frequency (for trials with the *F1 Ultra* infrared laser on metal only). Writing samples were generated with a font size of 2, 5, 10, 15, and 20 pt. The fonts used included a sans-serif print, script, and serif print font which were called *Lato, Great Vibes*, and *Elephant*, respectively (figure 4).

Figure 4: Example of microscopic image taken of writing test results on stainless-steel. Font names from top to bottom: Lato, Great Vibes, *and* Elephant

3.3.3. Line Tests

The line thickness test was used to aid in laser spot size determination. This is done by engraving lines of various thicknesses. The thicknesses are set to be very small - presumably thinner than the laser can possibly engrave. If the average line thickness of the lines of various sizes are equal to each other and not the specified line size, it can be assumed that the measured thickness is the smallest possible line the laser can engrave. Figure 5 depicts a sample of the line tests.
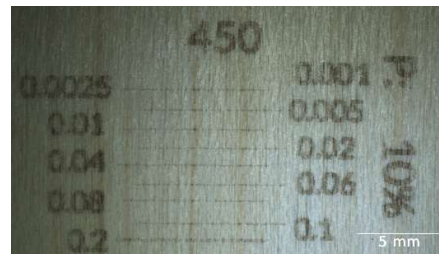

Figure 5: Example of microscopic image taken of the CO_2 laser line test with a speed of 450 mm/s and an output power of 10%

3.3.4. Color Tests

Because of the potential to mark metal with different colors relying only on laser-material interactions, an additional type of test referred to as the color tests were carried out on the metal samples.

The color tests included generating a matrix with various speeds on one axis and powers on the other. An example of these matrices is seen in figure 6Figure 6. These matrices were also repeated at various frequencies. The tests were carried out on both the stainless-steel sheets and the hybrid card samples. Both materials were examined for deformation, and in the case of the hybrid cards, the PVC on the back of the cards were observed for melting or burning. It is important to avoid using laser parameters on the hybrid card that affect the PVC due to PVC's hazardous properties when it burns. PVC begins to release hydrogen chloride when it reaches a temperature of 135° - according to Kudzin et al. - which poses a significant health and environmental risk [15]. Any deformation to either side of the material would also be very undesirable from the perspective of the customer.

Each test provides important insight into how the materials may react when trying to achieve different effects and designs. Figure 6 shows an example of a color test on an all-metal sample.
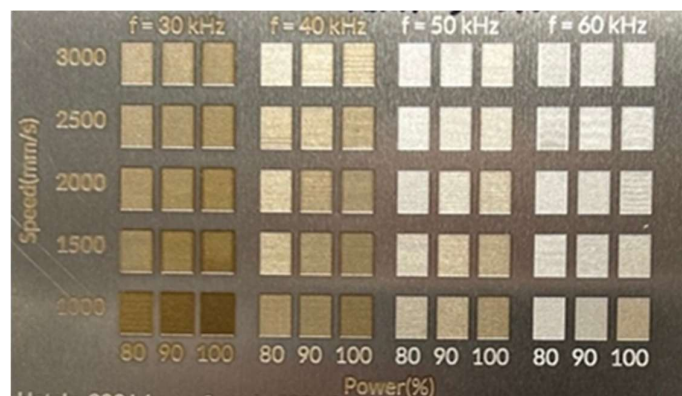

Figure 6: Example of color testing matrix

3.3.5. Infrared Tests

As for the wood, tests were carried out using the two infrared lasers to discover if radiation of this wavelength interacts with the maple wood. *Toppan* has an infrared laser at their disposal; therefore, it would be convenient if these lasers could be used to customize wooden payment cards.

3.4. Characterization

The following sections describe how the results were characterized, what criteria, equipment, and theoretical principles were used to do so.

3.4.1. Resolution Tests

The samples engraved with the resolution test template were examined both through the microscope and with the naked eye. Due to the application of payment cards, it is imperative that the engravings are clear and visible to the unaided eye thus, the final conclusions were determined exclusively through viewing the samples without the aid of the microscope. For each set of parameters, the smallest line width for which space between adjacent lines can still be seen was noted. This value was determined for the vertical, horizontal, and diagonal line patterns individually.

3.4.2. Writing Tests

Similarly, the writing test samples were also viewed under a microscope, and with the naked eye. Again, since the laser engravings are meant to be used as a means to customize payment cards, the results that are seen with just the naked eye are considered. Each writing sample was given a score of 1, 0.5, or 0 meaning the words are clear and legible, legible depending on the visual abilities of the viewer, or not legible, respectively. Reasons for a sample receiving a poor score include burning which leads to color bleeding around the text, color being too light, or inconsistent coloring within the characters.

3.4.3. Line Tests

The microscope images of the line tests were examined using the image processing software: *Image J*. This was done by measuring the line thickness of each engraved line at multiple points to find the average line thickness. This data was then compared to the specified line thickness which was input into *xTool Creative Space*. The line thicknesses were purposely set to very thin lines that were likely smaller than the laser would be able to resolve. Therefore, the line thickness that is extrapolated for all of these lines will end up being related to the laser spot size.

3.4.4. Color Tests

The color tests were examined with the naked eye and by collecting CIE L*a*b* color data to quantitatively compare colors. This data includes an L*, a*, and b* value for each colored sample. The distance between two colors described by these three values can be determined through the ΔE value [16, 17]. The CIE94 model was used for these calculations which uses elements from the CIE L*C*h* color space.

In addition to the L*, a*, and b* values previously mentioned, C* - chroma - is introduced in the CIE94 color model:

$$C^* = \sqrt{(a^*)^2 + (b^*)^2} \tag{6}$$

The ΔE_{94} value is calculated as follows [18]:

$$\Delta E_{94} = \sqrt{\left(\frac{\Delta L^*}{k_L S_L}\right)^2 + \left(\frac{\Delta C^*}{k_C S_C}\right)^2 + \left(\frac{\Delta H^*}{k_H S_H}\right)^2} \tag{7}$$

It uses the color difference value that is standard for the CIE76 color space –

$$\Delta E_{ab} = \sqrt{(\Delta L^*)^2 + (\Delta a^*)^2 + (\Delta b^*)^2} \tag{8}$$

- and the difference in luminous exposure, which can be written two ways [16, 19]:

$$\Delta H^* = \sqrt{(\Delta E_{ab})^2 - (\Delta L^*)^2 - (\Delta C^*)^2} \tag{9}$$

$$\Delta H^* = \sqrt{(\Delta a^*)^2 + (\Delta b^*)^2 - (\Delta C^*)^2} \tag{10}$$

The standard S, k, and K values used to analyse colors in the graphic arts include [19]: $S_L = 1$, $k_L = k_C = k_H = 1$, $K_1 = 0.045$, $K_2 = 0.015$,

$$S_C = 1 + K_1 C_1^* \text{, and} \tag{11}$$

$$S_H = 1 + K_2 C_1^* \tag{12}$$

Using this standard, the minimum color difference that will be perceived by the human eye – or just noticeable difference [JND] - is 1 [18].

The fluence of the laser for each color trial was calculated using the uniform density shape shown in the following formula:

$$F_{pulse} = P_{avg}/(f\pi w^2), \tag{14}$$

where F is the fluence [J/mm^2], P_{avg} is the average laser output power [W], f is the pulse frequency [Hz], and w is the laser waist [mm]. This data was used to determine if the color produced on the metal could be related to both laser speed and fluence.

An additional metric to describe fluence was introduced to determine which method of calculation provided the most accurate way to predict the resulting color. Accumulated fluence is a parameter which tells how much energy is irradiated on a specific area of the material [17]. The formula for accumulated fluence,

$$F_{acc} = P_{avg}/(vH), \tag{15}$$

still includes the average output power, P_{avg} in Watts, in addition to the laser velocity, v in mm/s, and the line spacing of the engraving, H [mm] [17]. The line spacing can be easily derived from the hatch value - which was a parameter in these trials - by taking its reciprocal.

The two fluence metrics were used so it could be determined which calculation method gave better insight into which color would be produced. Whichever metric showed the smallest color difference values between cells engraved with the same fluence would decidedly be the better metric.

Similarly, the writing test samples were viewed under the microscope and with the naked eye. Again, since the laser engravings are meant to be used as a means to customize payment cards, the results that are seen with just the human visual system are considered.

The samples were cleaned in an ultrasonic bath filled with demineralized water to remove debris and unwanted color effects that were produced due to something other than the laser - metal interaction. Each sample was left in the bath for five minutes.

4. Wood

4.1. Results and Discussion

The following sections present the results of the writing, resolution, and line tests for each of the three lasers used in the trials as well as the infrared laser trials. *Python* was used to analyze the numerical data, and *Microsoft Excel* was used to organize and present the qualitative observations.

4.1.1. P2S CO2 laser

The first trials were carried out with the CO_2 laser (*xTool P2S*).

The text produced by this laser has a halo effect when engraved at higher powers - as seen in figure 7. This could be due to heat traveling through the material and causing it to burn, or it could be smoke stains. It is relevant to note that obtaining a darker color without introducing haloing could be done by engraving with a lower power and with multiple passes. There were no wood trials completed as a part of this study which had multiple laser passes; although, they should be completed before an official recommendation of optimal laser parameters is given.
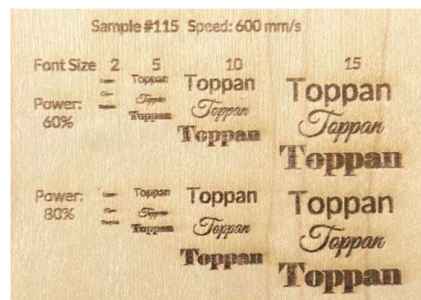

Figure 7: Discoloration surrounding the P2S laser

The results of the CO_2 laser writing test are presented in Table 5tables 5 and 6.

Power	10%			15%			20%			
Speed (mm/s)	300	400	500	300	400	500	200	300	400	500
Font Size (pt)										
2					0		0	0		
5					0.5		0	0		
7	1	0.5	0	1	0.5	0		1	0.5	0.5
10					1		1	1		
15					1		1	1		

Table 5: Writing test results for CO2 laser with hatch of 100 L/cm powers of 10, 15, and 20%

A font size of 2 pt is not legible when engraved on maple wood for any parameters or fonts used in these trials. The legibility of the font sizes depended less on the laser's parameters compared to the smaller font sizes.

Power	30%		40%		60%
Speed (mm/s)	500	600	500	600	600
Font Size (pt)					
2	0	0	0	0	0
5	0	0	0	0	0
7					
10	1	0.5	1	1	1
15	1	1	1	1	1

Table 6: Writing test results for CO2 laser with hatch of 100 L/cm powers of 30, 40, and 60%

The font size of 7 was engraved at various speeds and powers to examine if a hatch of 50 L/cm could be legible (table 7).

Power	10%	15%	20%
Speed	Hatch = 50 L/cm, Font Size = 7 pt		
300	0	0	0
350	0	0	0
400	0	0	0
450	0	0	0
500	0	0	0

Table 7: Writing test results for CO2 laser with hatch of 50 L/cm and font size of 7 pt

Apparently, there were no examples of a hatch of 50 L/cm creating legible text at a font size of 7 pt; therefore, a higher hatch value should be used.

Power of at least 30% should be used when engraving text onto wood with the *P2S* laser. A font size of at least 10 pt should be used as there is a lack of clarity with the smaller font sizes.
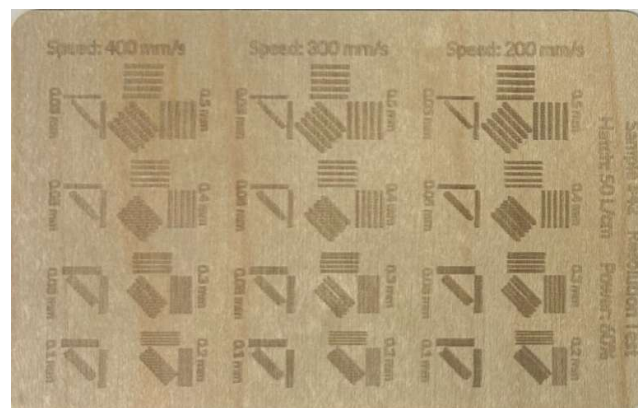

Figure 8: Resolution Test

In the results from the resolution test (figure 8Figure 8), the line orientations of vertical, horizontal, and at a 45° angle are differentiated by labeling the results with V, H, and D, respectively. The resolution appears to not be significantly dependent on the laser parameters but, it is more reliant on the orientation of the patterns. Table 8 shows the results for the resolution test with the *P2S* laser having an output power of 60%.

Hatch (L/cm)	50	50	50	50	50	50
Speed (mm/s)	200	300	400	450	500	550
Power	Minimum line width that can be resolved (mm)					
60%	V 0.2	V 0.2	V 0.2	V 0.2	V 0.2	V 0.2
	H 0.3	H 0.4	H 0.4	H 0.4	H 0.4	H 0.4
	D 0.4	D 0.5	D 0.5	D 0.5	D 0.5	D 0.5

Table 8: Resolution test results for CO2 laser

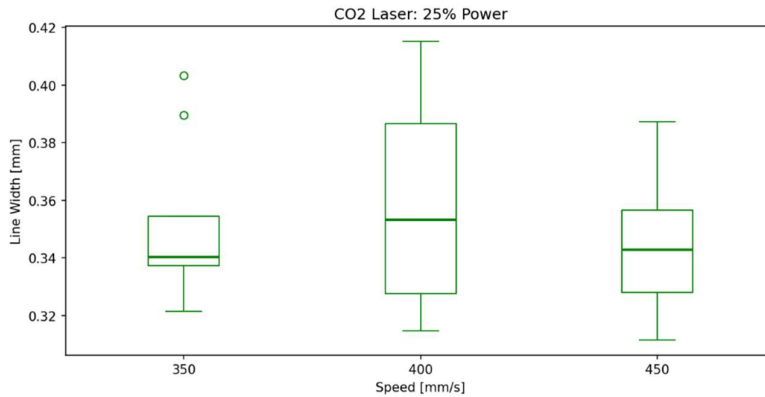| Speed (mm/s)	Line Width (mm)
350	0.351 ± 0.032
400	0.360 ± 0.042
450	0.344 ± 0.029
Average	0.352 ± 0.035

Table 9: CO2 laser line thickness results

Figure 9: The measured thickness of lines engraved by the CO_2 laser at a power of 25%

Figure 9 shows the measurements taken from the line tests carried out with the CO_2 laser running with an output power of 25%. These results suggest that for this specific laser - within the range of 350 to 450 mm/s - speed is not an important factor in the laser spot size. As seen in table 9, the average line width for the CO_2 laser is 0.35 ± 0.01 mm which is 0.20 ± 0.01 mm greater than the diameter of the laser beam when focused.

4.1.2. S1 Blue Laser

Following the completion of the CO_2 laser trials, the trials using the *xTool S1* blue diode laser began. The writing test produced results as seen in table 10Table .

The results of the *S1* blue laser writing tests were like those of the *P2S* CO_2 writing tests. Using larger fonts such as 10 or 15 pts would be favorable; however, using font size 7 pt at low speeds produces adequate results. These trials should be repeated at a wider range of speeds and powers to find the optimal parameters for engraving on this material.

Power		20%					35%		50%		75%	
Speed		100	200	300	400	500	300	500	300	500	500	600
Hatch	Font Size											
100	2						0	0	0	0	0	0
100	5						0.5	0	1	0.5	0	0
100	7	1	1	0.5	0.5	0						
100	10						1	1	1	1	1	1
100	15						1	1	1	1	1	1

Table 10: Writing test results for the S1 *blue diode laser*

Similar to the results seen with the CO_2 laser resolution test, the smallest line and space size that can be resolved is mostly dependent on the pattern orientation (table 11).

Hatch (L/cm)	100	50	100	50	100	50
Speed (mm/s)	200	200	300	300	400	400
Power	Minimum line width that can be resolved (mm)					
20%	V 0.2 H 0.2 D 0.3		V 0.2 H 0.3 D 0.3		V 0.2 H 0.3 D 0.3	
30%	V 0.2 H 0.3 D 0.4		V 0.2 H 0.3 D 0.4		V 0.2 H 0.3 D 0.4	
60%		V 0.2 H 0.2 D 0.5		V 0.2 H 0.2 D 0.5		V 0.2 H 0.2 D 0.5

Table 11: Resolution test results for S1 *blue diode laser*
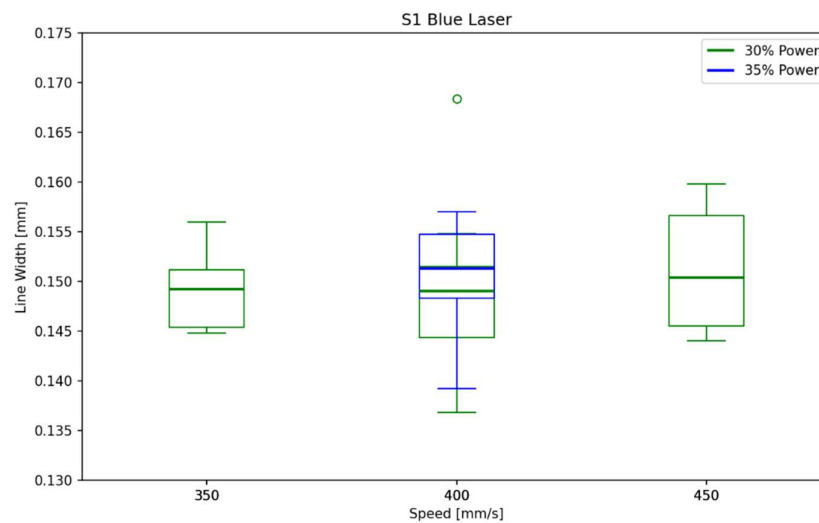

Figure 10: The measured thickness of lines engraved by the S1 *blue diode laser*

Both the results from the blue diode laser running with an output power of 30 and 35% are shown in figure 10. Line tests were only run at the output power of 35% for a speed of 400 mm/s. By comparing the results from both powers at a speed of 400 mm/s, one can see that there isn't great variation in the line width between the two tests although the lines that were created with a higher power tend to be thicker. This result seems intuitive; however, the power difference between the two datasets is quite small and the difference could be due to a lack of data points. More trials need to be completed with a broader range of powers to verify if this is a real effect.

Speed (mm/s)	Line Width (mm)
350	0.149 ± 0.007
400	0.150 ± 0.011
450	0.151 ± 0.010
Average	0.150 ± 0.010

Table 12: S1 blue diode laser line thickness results for a power of 30%

The average line thickness produced by laser engraving with the blue diode laser at an output power of 30% was measured to be 0.15 ± 0.01 mm (table 12).

Speed (mm/s)	Line Width (mm)
400	0.151 ± 0.009

Table 13: S1 blue diode laser line thickness results for a power of 35%

Table 13 depicts the average line thickness of 0.15 ± 0.01 mm for a speed of 400 mm/s. This value is 0.05 ± 0.01 mm larger than major diameter of the spot and 0.07 ± 0.01 mm larger than the minor diameter of the laser's spot.

4.1.3. F1 Ultra Blue laser

Finally, the *F1 Ultra* blue diode laser was used to complete the writing, resolution, and line thickness tests.

Based off the results depicted in table 14, this laser - at least with these specified parameters - is not well equipped to produce clear writing at a font size of 2, 5, or 7 pt.

Power		70%				100%			
Speed		300	500	600	1000	400	600	1000	1200
Hatch	Font Size								
100	2	0	0	0	0	0	0	0	0
100	5	0	0	0	0	0	0	0	0
100	7	0.5	0.5	0					
100	10	1	1	0.5	0.5	1	1	1	1
100	15	1	1	1	1	1	1	1	1

Table 14: Writing test results for the F1 blue diode laser

Regarding the resolution test, this laser provides the most clarity that the lasers resolution is a function of the orientation of the design being engraved rather than parameters including power or speed. For each combination of power and speed tested during these fiber laser trials, the minimum line pattern that could be resolved is consistent for each pattern orientation (table 15).

Hatch (L/cm)	100	100	100
Speed (mm/s)	600	800	1000
Power	Minimum line width that can be resolved (mm)		
60%	V 0.2 H 0.3 D 0.4	V 0.2 H 0.3 D 0.4	V 0.2 H 0.3 D 0.4
70%	V 0.2 H 0.3 D 0.4	V 0.2 H 0.3 D 0.4	V 0.2 H 0.4 D 0.4
80%	V 0.2 H 0.3 D 0.4	V 0.2 H 0.3 D 0.4	V 0.2 H 0.3 D 0.4

Table 15: Resolution test results for F1 blue diode

The F1 blue laser was used to engrave lines at output powers of both 60 and 70% and speeds of 350, 400, and 450 mm/s. Figure 11 displays the results of these tests. Contrasting the results of the previously discussed lasers, it is clear that engraving at a higher power led to thicker line widths. Additionally, the speed appears to be inversely proportional to the engraved line thickness. These results are in line with the thermal effects the laser has on the wood.
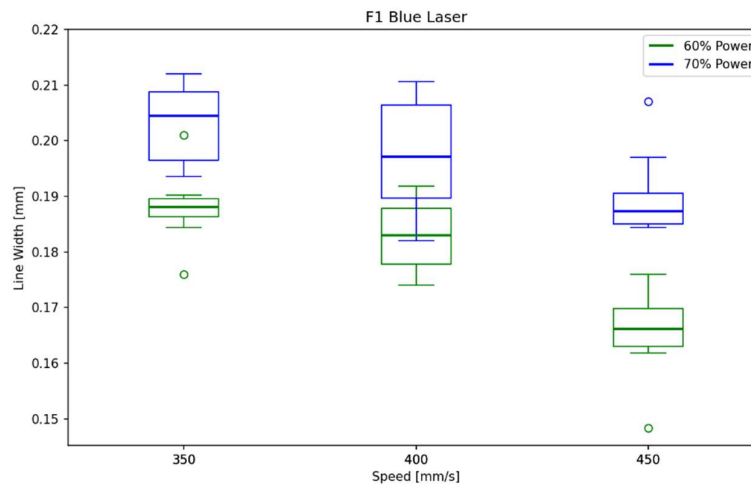
Figure 11: The measured thickness of lines engraved by the F1 blue laser

According to tables 16 and 17, the average line thicknesses are 0.18 ± 0.01 mm and 0.20 ± 0.01 mm, respectively. For trials run at a power of 60%, the line thickness is 0.10 ± 0.01 mm or 0.08 ± 0.01 mm larger than the two given diameters of the elliptical spot. At a power of 70%, the average line thickness is 0.12 ± 0.01 mm or 0.10 ± 0.01 mm larger than the elliptical spot size of the *F1 Ultra* blue laser.

Speed (mm/s)	Line Width (mm)
350	0.188 ± 0.010
400	0.183 ± 0.013
450	0.166 ± 0.014
Average	0.179 ± 0.016

Table 16: F1 blue laser line thickness results for a power of 60%

Speed (mm/s)	Line Width (mm)
350	0.203 ± 0.013
400	0.198 ± 0.018
450	0.190 ± 0.013
Average	0.197 ± 0.016

Table 17: F1 blue laser line thickness results for a power of 70%

4.1.4. Infrared Lasers

Multiple trials were carried out using the *xTool F1 Ultra* infrared fiber laser on the wooden cards. Parameter test matrices were generated with speeds ranging from 100 to 600 mm/s, a hatch of 100 L/cm and the power ranging from 50 to 100%. These test matrices were set to engrave on the wood at pulse frequencies of both 30 kHz and 60 kHz. No change to the material was observed, therefore another test matrix was generated.

This second matrix had speeds ranging from 50 to 100 mm/s, a hatch of 100 L/cm, and powers between 50 and 100% and a frequency of 60 kHz. In this case, markings were made on the wood towards the higher power and slower speed corner of the matrix (figure 12).
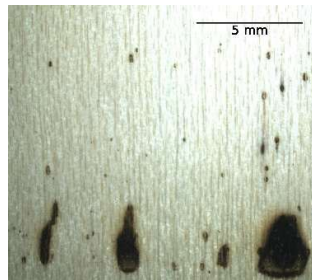

Figure 12: Test attempt to mark maple wood with an xTool infrared laser beam

Next, a trial was done using the *Otto Kuennecke* laser. Three test patches were created: those with a frequency of 100 kHz, speed of 100 mm/s, a hatch of 200 L/cm, and powers of 85, 90, and 100%. The lowest power had no effect on the wood; however, burning occurred during the trials with higher powers. The trials carried out at 90 and 100% power are seen in figure 13.
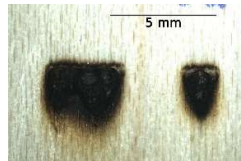

Figure 13: Test attempting to mark maple wood with an Otto Kuennecke YAG diode infrared laser

The CO_2 and both blue lasers provide favorable results for engraving on wood. Any of these three lasers could be used to add customizations to wooden payment cards. Both the *Otto Kuennecke* and the *F1 Ultra* fiber laser proved to be unable to produce any results that would be interesting for this application.

The following sections discuss the general trends observed for each type of test on the wood cards along with potential explanations for why these trends may occur.

4.1.5. Writing Test

In general, the samples that were given a rating of 0.5 or 0 were too light to be read at a distance or they were burnt which was seen by color bleeding around the word or inhomogeneous coloring which lent to the word being less clear (figures 14 and 15).
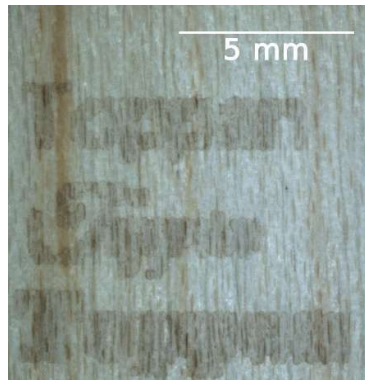

Figure 1413: CO2 laser test at speed of 450 mm/s with a hatch of 50 L/cm

Figure 1514: Diode laser test at speed of 100 mm/s with a hatch of 200 L/cm

It can be deduced that a hatch of 50 L/cm should not be used to engrave text since in all cases examined during these tests, none of the results with this parameter were considered sufficiently legible. Hatch should be set to at least 100 L/cm to provide uniformity throughout the engraving.

Speed has a significant impact on the clarity of the engraved text. The slower the speed, the clearer and darker the engravings are. At very fast speeds, the engravings become illegible although this is more seen at lower powers. Visually, this is because the color produced by the laser using these parameters does not have enough contrast from the background color of the maple wood. Engravings with higher powers can produce legible results at higher speeds.

Additionally, these results allow for the conclusion that the combination of the *Great Vibes* font at a size of 7 pt or lower is never sufficient for use on a payment card because the results are not legible. If this font, or another script type font, is desired to be used, it is recommended to make the font larger. This conclusion should pose no problems because any integral information written on a payment card will be written in print. Any words written in script will be purely stylistic.

4.1.6. Resolution Test

From the results of all three lasers, it can be concluded that the resolution is something that is unique to the laser and is not generally affected by the input parameters of the laser. Rather than a difference in resolution between trials with different parameters, a difference is seen between line patterns of different orientations within trials with the same parameters. There are two main explanations for why this may occur.

The first explanation is seen in figure 16 which depicts how the variation in laser motion relative to the line orientation plays a role in resolution. When the laser path is parallel to the orientation of the lines, the laser can produce a higher resolution. This suggests that the resolution is dependent on the direction of laser motion relative to the pattern orientation.
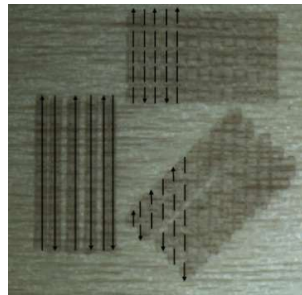
Figure 16: The direction of laser motion in the bi-directional laser motion setting

The second potential explanation is that the difference in resolution is due to elliptical spot sizes (figure 17). The website of the laser manufacturer claims that both the *S1* and *F1 Ultra* blue lasers have elliptical spot sizes [10]. This could explain how in the resolution tests using these lasers, the resolution in one direction is better than the resolution of the other direction.
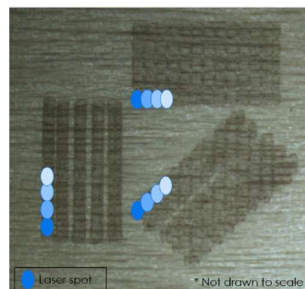

Figure 17: Engraving with non-symmetrical laser spots

27

4.1.7. Line Test

All line test trials, regardless of the laser used, exhibited the gaussian profile as described by Chernykh et al. [5]. This effect made collecting the line thickness data challenging because often times it was not clear as to what should be considered the boarder of the line. For this reason, five measurements were taken for the thickness of each line which were then averaged.

Table 18 lists the average line width of each laser model which was calculated from all the data collected for each laser (regardless of parameters). Based on the results found by averaging the width of all line tests done by each laser, it was determined that the *S1* blue diode laser had the smallest spot size because it was able to consistently produce the smallest line width. The average width of the *F1* laser lines was clearly larger than that of the *S1* laser however, these two lasers had the same spot size [10]. This discrepancy could lend itself to the *F1* laser not being correctly focused.

Laser	Line Width (mm)
CO_2	0.352 ± 0.035
S1 Blue	0.150 ± 0.009
F1 Blue	0.188 ± 0.018

Table 18: Average line width measured for each laser model

On the other hand, it was deduced that the CO_2 laser had the largest spot size which was almost double the average line width of the fiber laser. This result is to be expected because the nominal spot size of the *P2S* laser model is the largest of the three used in these tests.

A limiting characteristic of this medium is the grain of the wood. For engravings of lighter colors, the non-uniformity of the materials natural coloring can lead to decreased contrast between the material and the engravings.

4.1.8. Infrared Lasers

Both the YAG diode and the fiber infrared lasers used in these trials appear to be unsuited to produce any sort of design or text on the maple wood cards. The infrared lasers have no effect on the wood until burning occurs which appears to start from within the material rather than the surface. This suggests that it is the glue within the wood card that is being affected by the laser and not the wood itself.

4.2. Comparison and Recommendations

According to the trials carried out on maple wood cards with the *xTool P2S*, *S1*, and *F1 Ultra* lasers, there are some recommendations that should be kept in mind for the application of these results.

It is recommended that more tests be carried out to fully understand the interactions between the wood samples and each laser. Principally, the resolution tests should be repeated with different pattern orientations to determine what is causing the resolution discrepancies.

Primarily, it is recommended that the hatch settings of each laser be set to at least 100 L/cm. These values seem to provide an even color throughout the engravings in most cases. One should avoid using a hatch of 50 L/cm because the engravings tend to turn out too light, and the striation from the laser can be seen within the engravings since they are so far apart.

Next, one should use a font size of at least 7 pt when engraving on this material. There are cases where a font size of 5 is clear and legible; however, due to the natural variations in the color and the grain of the wood it is better to use a larger font.

Ultimately, either of the blue lasers are recommended to be used to engrave on maple wood because they have a smaller spot size and produce a better resolution. Yet, the CO_2 can produce adequate results.

Upon examination of all results, it was determined that the three lasers - including the *xTool P2S* CO2, *S1* blue, and *F1 Ultra* blue lasers - provided sufficient results when engraving on wooden cards. The two infrared lasers used in the study will not be able to be used for laser engraving on maple wood.

5. Stainless Steel

5.1. Results and Discussion

After processing the material, a halo effect was observed surrounding the engraved areas - particularly those engraved with a low frequency. The effect can be seen in figure 18 which shows that it can provide a decreased visual resolution and sharpness of the engraving. It was found that these markings can be easily removed by cleaning the surface of the metal with some cleaning product and a lint free cloth; however, this process also removed some of the color within the engravings.
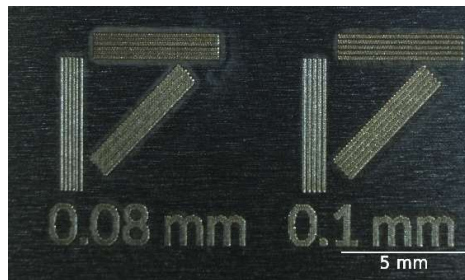
Figure 18: Discoloration of the material can be seen surrounding the engravings

In order to remove the unwanted halo effects - and any other effects that are caused by dust or debris - the ultrasonic bath is used to clean all samples uniformly. One metal sample before and after cleaning is shown in and figures 19 and 20. The figures show that the colors of the engravings are less gold and more silver after the cleaning.
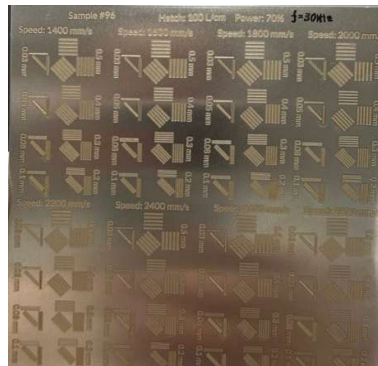
Figure 19: Metal sample before cleaning in the ultrasonic bath

Figure 20: Metal sample after cleaning in the ultrasonic bath

Additionally, something that cannot be seen very well in the image is the new inconsistency in the color of the engravings after cleaning.

Figures 21 and 22 show a comparison between a color test sample on a hybrid card before and after cleaning in the ultrasonic bath. The color removing effect is much more evident in the color test samples.
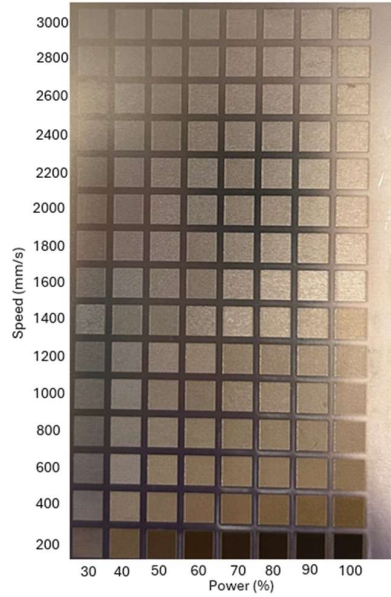

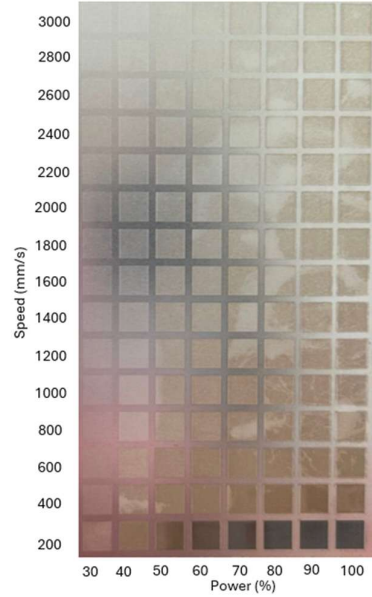Figure 21: Hybrid sample before
cleaning in the ultrasonic bath

Figure 22: Hybrid sample after
cleaning in the ultrasonic bath

5.1.1. Resolution Tests

As seen in table 19 and 20, the results for each resolution test were compiled and each resolution pattern is given the smallest line pattern size that was able to be resolved for the vertical [V], horizontal [H], and 45° [D] directions. The results are quite similar regardless of pulse frequency, laser speed, and power. Notably, the line patterns with a vertical or horizontal orientation have a better resolution compared to the line pattern at a 45° angle relative to the laser motion.

Frequency (kHz)	30	30	30	30	30	30	30	30
Speed (mm/s)	1400	1600	1800	2000	2200	2400	2600	2800
Power	Minimum line width that can be resolved (mm)							
70%	V 0.05 H 0.05 D 0.1	V 0.05 H 0.05 D 0.1	V 0.05 H 0.05 D 0.1	V 0.05 H 0.05 D 0.1	V 0.08 H 0.05 D 0.1	V 0.08 H 0.05 D 0.1	V 0.08 H 0.05 D 0.1	V 0.08 H 0.05 D 0.1
80%	V 0.05 H 0.05 D 0.1	V 0.05 H 0.05 D 0.1	V 0.05 H 0.05 D 0.1	V 0.05 H 0.05 D 0.1	V 0.08 H 0.05 D 0.1	V 0.08 H 0.05 D 0.1	V 0.08 H 0.05 D 0.1	V 0.08 H 0.05 D 0.2

Table 19: Results of resolution test for a frequency of 30 kHz

31

Frequency (kHz)	40	40	40	40	40	40	40	40
Speed (mm/s)	1400	1600	1800	2000	2200	2400	2600	2800
Power	Minimum line width that can be resolved (mm)							
70%	V 0.05 H 0.05 D 0.2	V 0.05 H 0.05 D 0.2	V 0.05 H 0.05 D 0.2	V 0.05 H 0.05 D 0.2	V 0.05 H 0.05 D 0.2	V 0.05 H 0.05 D 0.2	V 0.05 H 0.05 D 0.2	V 0.05 H 0.05 D 0.2
80%	V 0.05 H 0.05 D 0.1	V 0.05 H 0.05 D 0.1	V 0.05 H 0.05 D 0.1	V 0.05 H 0.05 D 0.1	V 0.05 H 0.05 D 0.1	V 0.05 H 0.05 D 0.1	V 0.05 H 0.05 D 0.08	V 0.05 H 0.05 D 0.1

Table 20: Results of resolution test for frequency of 40 kHz

A very small difference in the resolution of the diagonal pattern is observed when the power is at 70%. As the frequency increases from 30 to 40 kHz, the minimum line width which can be resolved changes from 0.1 to 0.2 mm (for the diagonal pattern). This change is quite small but should still be noted.

The resolutions found through all resolution tests on this material are quite good.

On average the resolution for the vertical and horizontal patterns are 0.05 mm, and the resolution for the diagonal pattern is 0.1 mm.
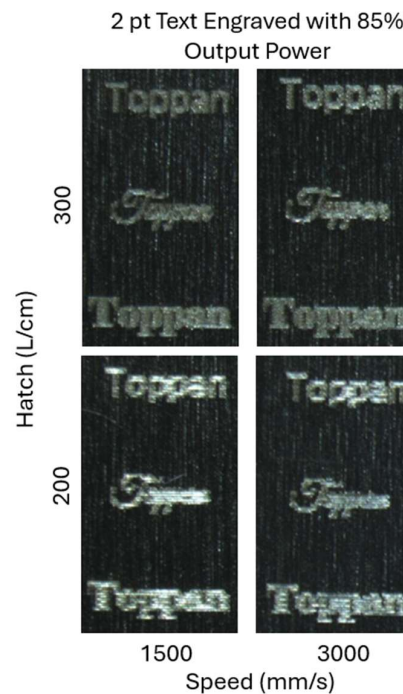
5.1.2. Writing Tests

Figure 23: Font size of 2 pt engraved on all metal samples with an output power of 85%

32

All writing tests proved to produce clear and legible results with the exception of the words written in script with the smallest font size. Additionally, the words written with the same font size (2 pt) were difficult to read with only the naked eye, although the two other iterations of 'Toppan' written in print were clearly legible with the aid of the microscope. Figure 23 shows writing tests engraved with hatch values of 200 and 300 L/cm and speeds of 1500 and 3000 mm/s, engraved at 85% output power.

There was no significant difference between the tests with different parameters besides the color of the writing. Specifically, the tests performed with a lower pulse frequency tended to be a bronze color while the tests with a higher pulse frequency produced white or silver writing. These results are consistent with those found in the color tests.

Introducing the writing samples to the ultrasonic bath cleaning method changed the color of the text and decreased the halo effect observed in the pre-cleaned sample. Figures 24 and 25 show a portion of a writing test which was engraved on an all-metal sample with an output power of 85%, laser speed of 2000 mm/s, hatch of 200 L/cm, and a frequency of 60 kHz. These figures show the same portion of the sample before and after cleaning. The color difference and overall change in clarity that was accomplished by cleaning the sample. The apparent change in color of the background was not apparent visually and is therefore due to a difference in lighting conditions at the time which the photos were taken.

Figure 24: Writing test sample pre-cleaning in an ultrasonic bath. Font sizes of 10 pt and 15 pt

Figure 25: Writing sample post-cleaning in an ultrasonic bath. Font sizes of 10 pt and 15 pt.

5.1.3. Line Tests

As seen in tables 21, 22, and 23, there is a general trend of line width increasing with both power and speed.

Power	Average Line Thickness (mm)
60%	0.076 ± 0.004
70%	0.086 ± 0.004
80%	0.098 ± 0.002
90%	0.091 ± 0.007

Table 21: Line thickness measurements for a line with specified thickness of 0.0025 mm and laser speed of 1500 mm/s

Power	Average Line Thickness (mm)
60%	0.092 ± 0.005
70%	0.088 ± 0.014
80%	0.109 ± 0.001
90%	0.094 ± 0.006

Table 22: Line thickness measurements for a line with specified thickness of 0.0025 mm and laser speed of 2000 mm/s

Power	Average Line Thickness (mm)
60%	0.091 ± 0.007
70%	0.096 ± 0.012
80%	0.115 ± 0.005
90%	0.113 ± 0.003

Table 23: Line thickness measurements for a line with specified thickness of 0.0025 mm and laser speed of 2500 mm/s

Based on these results, the average minimum spot size is 0.096 mm with a standard deviation of 0.013 mm. According to the laser manufacturers website, the spot size of this laser is 0.03 x 0.03 mm. With this being said, the smallest lines engraved by this laser deviate from the minimum spot size by a maximum of 282%.

5.1.4. Color Tests

A variety of colors were able to be produced by varying the laser speed, power, and frequency. These colors include brown, gold, silver, white, and a mirror effect which can be seen in the hybrid card samples in figure 26 as well as colors such as blue, green, purple, and red which are seen in figure 27.
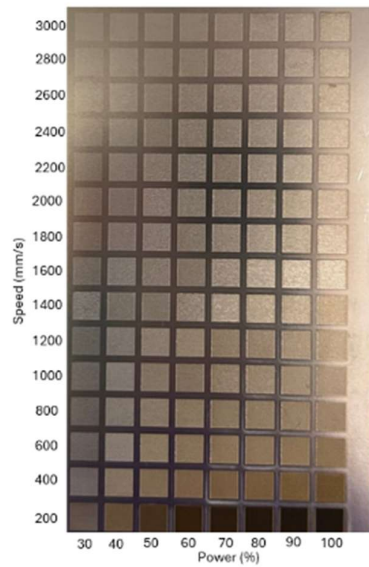
Figure 26: Range of colors produced on the hybrid card samples at a frequency of 40 kHz
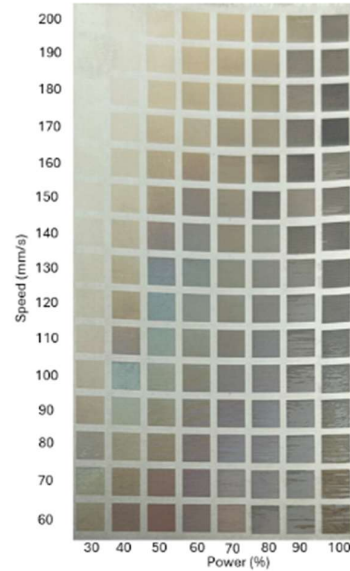

Figure 27: Range of colors produced on the hybrid card samples at a frequency of 60 kHz

The patches engraved with the high speeds, high power, and high frequencies and multiple laser passes do not appear to have a color change but, the surface seems to be polished by the laser - creating the mirror effect as seen in figure 28.
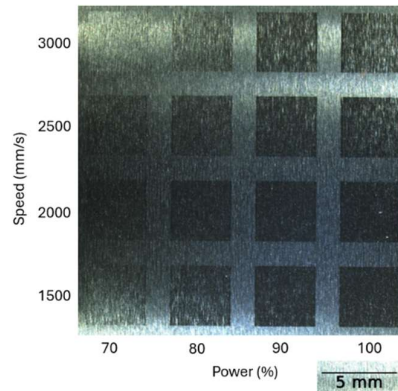

Figure 28: Mirror effect

35

As the power increases and the speed decreases, the patches turn to silver, white, gold, then become progressively darker. If the frequency and power of the laser is high enough, and the speed is slow enough, the patches stop growing darker and they appear to be colored with other colors such as reds, greens, and blues. The appearance of these colors are a result of laser marking – contrasting the previous laser engraving. The color that was observed depended on the laser parameters and changed slightly with the viewing angle.

Figures 29 and 30 show the same power, speed, and frequency parameters tested on both the full metal and the hybrid card test samples. For these parameters, the two samples did not produce the same colors. Additionally, the hybrid card sample shows greater inconsistency within each test patch compared to the full-metal sample. One possible explanation is that the PVC acts as an insulator for the heat generated by the laser. With this being said, the hybrid card sample will not be able to reach the same temperatures under the same conditions. As temperature plays a large role in laser marking, the effect of the insulator on the colors produced on the metal is great.
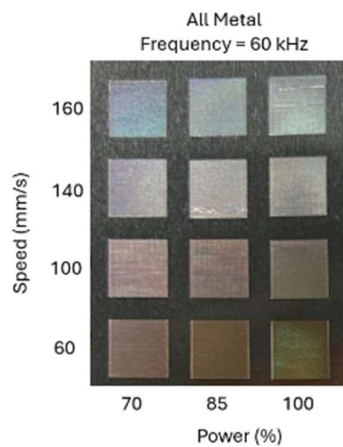

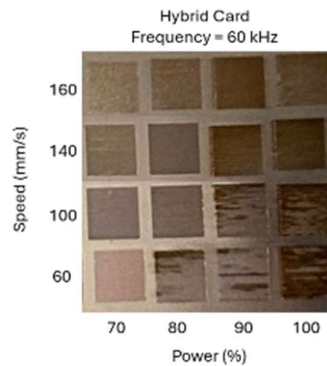Figure 29: Laser marking on stainless steel sample

Figure 30: Laser marking on hybrid card sample

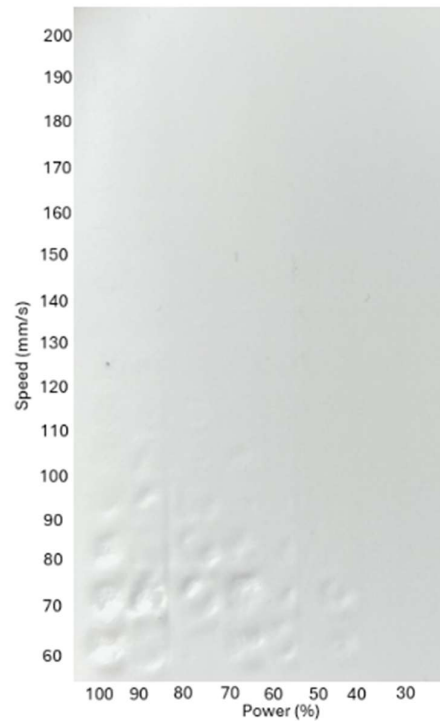*Figure 31: Deformation of hybrid card as a result of laser marking*

Figure 32: PVC melting on the reverse side of the hybrid card due to laser marking

When engraving with such high powers and low speeds, both the hybrid and the full-metal samples became deformed. Melting of the PVC occurred on the back side of the hybrid cards when they were engraved in this way (figures 31 and 32) Only the trials which attempted to produce color generated samples that had melting or warping.

The combinations of parameters used in these hybrid card tests and the calculated laser fluence values which resulted in the melting of the PVC are shown in table 24. This accumulated fluence values associated with the PC melting range from 133 to 333 J/mm^2.

Power	Speed (mm/s)	Freq (kHz)	Fluence/Pulse (J/mm^2)
100%	60-120	60	0.118
90%	60-120	60	0.106
80%	60-110	60	0.094
70%	60-100	60	0.083
60%	60-90	60	0.071
50%	60-70	60	0.059

Table 24: Parameters that caused PVC melting in hybrid cards

The full metal samples also experienced warping and unwanted effects on the back side of the material. The parameters and fluence per pulse that had this effect are shown in table 25. The accumulated fluence for these same parameters range from 140.0 to 2000.0 J/mm^2.

Power	Speed (mm/s)	Freq (kHz)	Fluence/Pulse (J/mm^2)
100%	20-200	60	0.118
85%	20-200	60	0.100
70%	20-200	60	0.083
100%	20-200	30	0.236
85%	20-200	30	0.200
70%	20-200	30	0.165

Table 25: Parameters that caused warping to the stainless-steel samples

The following plots are used to visualize the relationship between laser speed, accumulated fluence, and material damage. The figures include the parameters of all color test trials. The data is categorized into whether or not the parameters caused visible warping or melting to the material. Data points which caused these negative effects are denoted by a star.

Figure 33 visually compares the calculated data points of accumulated fluence and speed. The plot shows a clear logarithmic type trend. Along with this trend, it seems to be that there is a certain threshold which separates the parameters which caused negative effects on the material and those that didn't.

It is evident that accumulated fluence is indeed linked to whether the material will become damaged during the marking process as all of the data points experiencing such effects are positioned above a certain threshold on the y-axis.
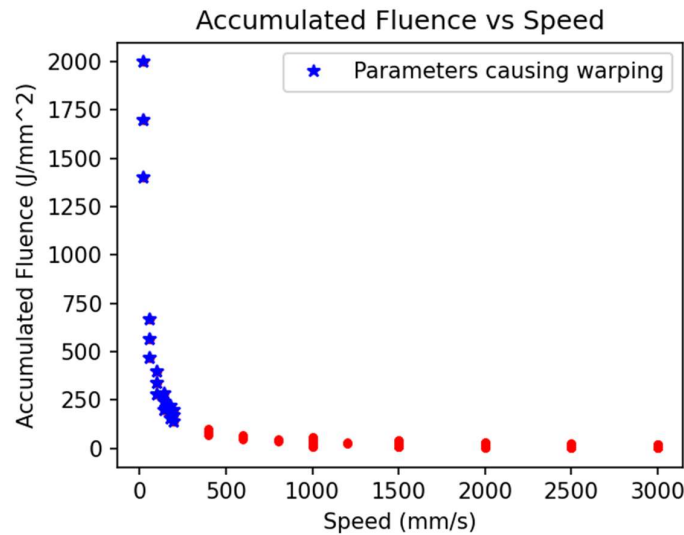

Figure 33: Accumulated fluence vs speed for the stainless-steel samples

Similarly to the stainless-steel samples, the accumulated fluence vs speed plot (figure 34) shows a logarithmic type of relationship between the two variables. Again, it appears that the parameters with negative effects are concentrated in one area of the plot where accumulated fluence is high and speed is low. The second plot, comparing fluence per pulse and power, shows a linear relationship. There are no clear conclusions to be drawn from this plot as there are not enough data points to recognize a further relationship between the variables.
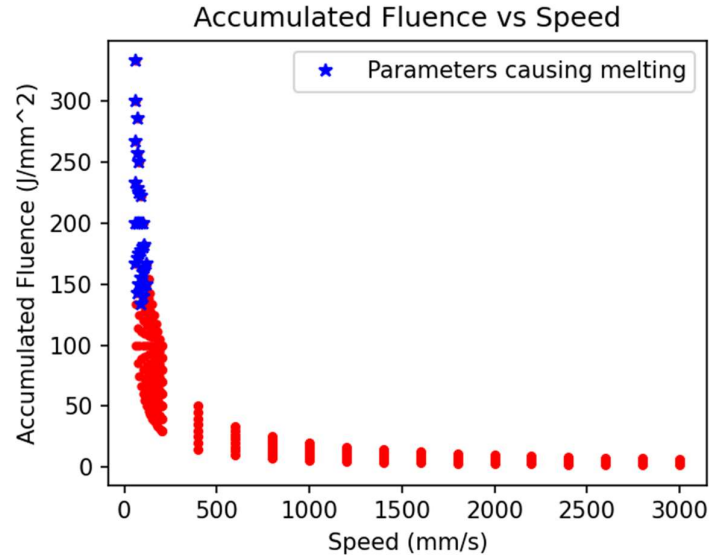
Figure 34: Accumulated fluence vs speed for the hybrid card samples

In an attempt to observe the trend related to observed color and technical chromaticity coefficient as suggested by Veiko et al., the values of the parameters used in these calculations are seen in table 26. The values listed are assumptions or approximations due to the information being unavailable or unspecified for the particular material or laser. The remaining parameters were specific to each trial and each test cell. A plot of this metric was generated for the data obtained by the color tests on the hybrid samples (figure 35). Each data point is colored according to the color which the cell exhibits visually. In the cases where multiple colors were present in one cell, or the color of the cell changed due to viewing angle, the dominant color was chosen.

Parameter	Value
Metal Reflectivity at λ = 1.06 μm (R)	0.75
Thermal conductivity (k)	0.24 [W/cmK]
Thermal diffusivity (a)	0.043 [cm^2/s]
Pulse Duration (τ)	50 [ns]

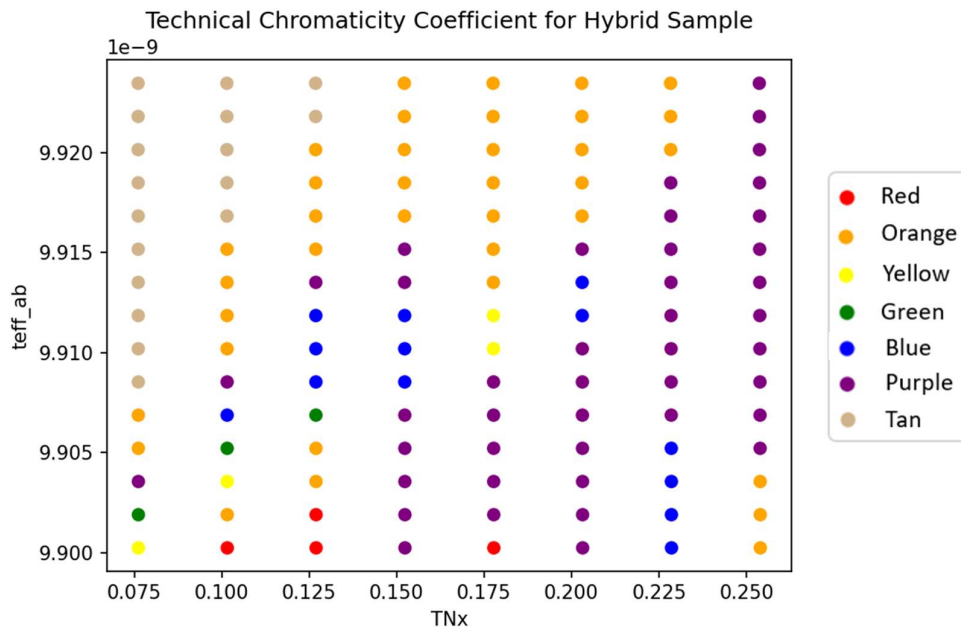*Table 26: Parameters used in the calculation of the technical chromaticity coefficient*

Figure 3515: Plot depicting the technical chromaticity coefficient for color tests on hybrid card samples

There is a general trend observed in the technical chromaticity coefficient plot; however, it is not the expected one. There are certainly groupings of colors suggesting that one can predict the color that will appear on the metal based on their effective time and maximum temperature values yet, the relationship is not simply multiplying these two values as suggested by equation 1.

Certainly, more data points are required to make a thorough conclusion. It is possible that the true trend is not yet evident as these values have only been taken from one color test sample. As previously stated, there are multiple parameters used in this calculation which were assumed. This could clearly play a role in inaccurate results.

Further, it was attempted to further characterize the color of the irradiated metal surface through the use of colorimetry.

The CIE L*a*b* color values collected with the *x-Rite* spectrophotometer only show a range of tans, grays, and brows; therefore, it would be justified to say that the spectrophotometer does not accurately capture the nuances of the colors that are able to be produced on the metal. Figures 36, 37, 38, and 39 allow for a comparison between the simulated colors based on the CIE L*a*b* values and the colors that are detected visually.
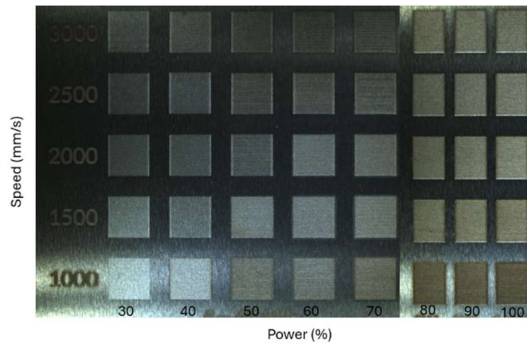
41

Figure 36: Colors produced on stainless steel samples with a pulse frequency of 30 kHz
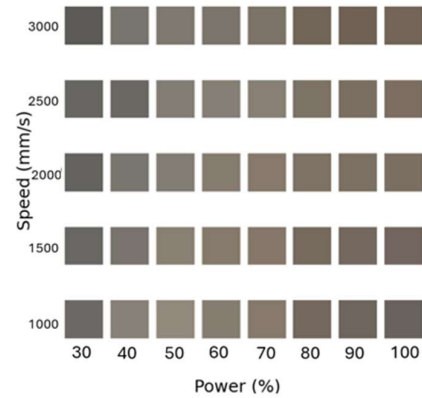

Figure 37: Simulated colors based on data collected from the sample shown in Figure
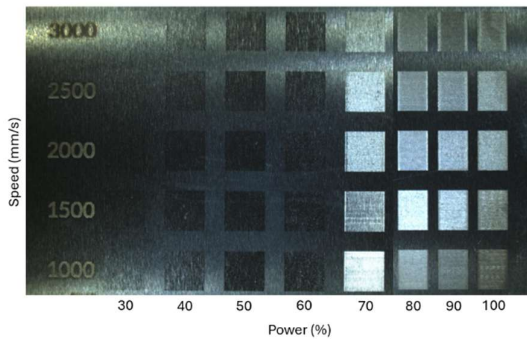

Figure 38: Colors produced on stainless steel samples with a pulse frequency of 60 kHz
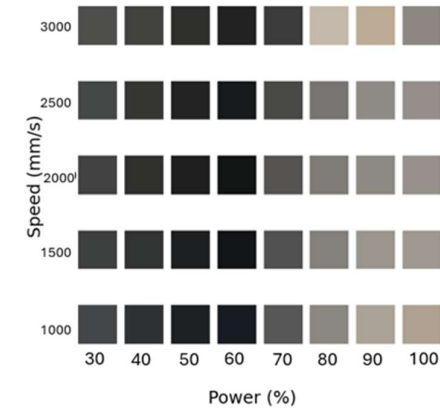

Figure 39: Simulated colors based on data collected from the sample shown in Figure

As previously stated, the spectrophotometer was not able to accurately detect the colors that were present on the metal due to the laser marking. To further this point, figure 40 compared the colors produced on the stainless-steel sample to the colors that were produced using the L*, a*, and b* values that were obtained with the *x-Rite* spectrophotometer. Evidently, the simulated colors are not at all representative of the colors that can be observed in the image of the sample.
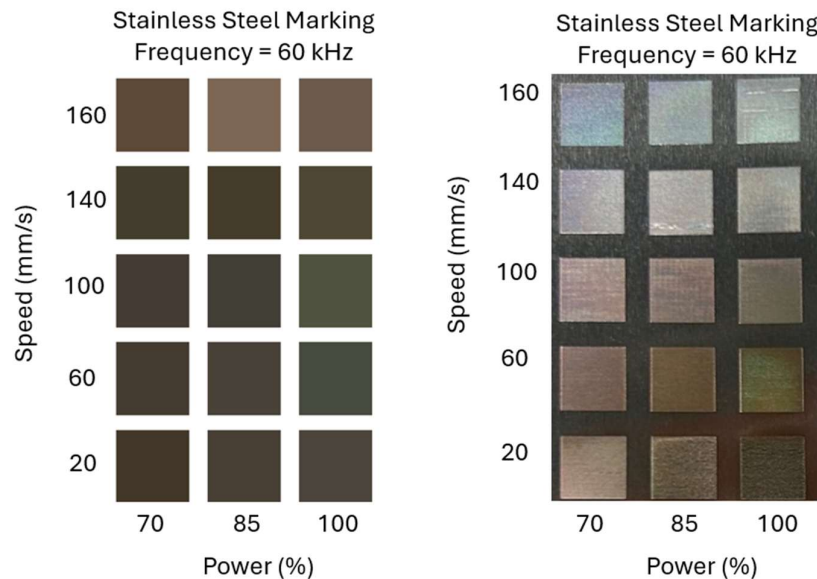
Figure 4016: Comparison between colors produced by simulating the L, a*, and b* values in Python and colors seen in an image of the color marked stainless-steel sample*

During these trials, as the frequency was increased, the threshold for the minimum power that produced a matte engraving increased. Matte engravings are of interest in this application because this would allow for the engravings to be distinguishable to the viewer from many viewing angles.

The combination of this material and laser has a rather impressive resolution. As previously stated, the shape of the laser spot is symmetrical - this could explain why the resolution of horizontal and vertical lines engraved with the same parameters were generally the same. The slight decrease in resolution associated with the diagonal line patterns could be due to the lasers path of motion while it is engraving however, this is only speculation further examination into this topic is required.

All of the writing tests provided extremely clear and legible results for the font sizes that may be used to decorate payment cards. The font size of 2 pt had some clarity issues but, engraving on payment cards with this font size would not be practical anyway because no matter the resolution, this font size is too small for most people to read.

As seen in the previous section, the measured line thickness generally increases with laser power. Interestingly, it was noticed that the measured line thickness tends to increase as speed increases. These results are to be expected for power; however, it would be expected that the laser makes a more precise engraving with higher speeds. The slower the laser speed, the more time the laser beam is in contact with a specific spot on the material surface; therefore, the laser should have a more intense effect on the stainless steel.

The laser spot size that was produced was significantly larger than the dimensions of the spot provided by the manufacturer. Assuming the laser beam is well aligned, and it is true to size, the additional line thickness could be due to the interaction between the metal and the laser. Even if the laser is not directly in contact with the metal, the adjacent particles will also be heated and changed by the interaction.

With this being said, the *xTool F1 Ultra* infrared laser can be used to engrave on stainless steel with high precision. This type of laser has great potential to be used to add information and customization to payment cards with stainless steel surfaces.

The infrared laser was able to produce a large variety of colors on the stainless-steel including pink, red, yellow, green, blue, and purple. The colors were produced when the laser had only the slowest speeds, highest pulse frequency, and highest power. With that being said, producing these colors also lead to unwanted effects on the material such as deformation. Otherwise, colors such as silver, gold, and brown were seen - which could be expected.

The *x-Rite* spectrophotometer was not able to detect every color produced by the laser-metal interaction. This is likely because the colors are only seen when viewed from certain angles. It is likely that the measurement geometry of this device does not permit these colors to be seen.

Additionally, due to the high reflectivity of the stainless steel, it is also likely that the reflection of the illuminant back to the mechanism interferes with the reading.

Both the fluence per pulse and the accumulated fluence of each cell which also had color data collected were calculated. These values were then used in combination with the CIE94 color difference model in an attempt to correlate the colors produced on the metal with either one of the fluence metrics.

These values were found through the following method: the data was split into groups of equivalent fluence with a precision of 0.00005 J/mm². The color difference was calculated between the color of each cell in the the specified group. These color difference value were then averaged within each group giving one color difference value per fluence value. Finally, an average was taken of all of the average color difference values to find a single average value for all of the data. This process was repeated for the two fluence metrics and for each material. The results are seen in tables 27 and 28.

	ΔE_{min}	ΔE_{avg}	ΔE_{max}
Fluence per Pulse	8.97	10.02	10.27
Accumulated Fluence	3.53	8.42	13.60

Table 27: CIE94 color difference values between colors engraved on stainless-steel samples with the same fluence

As evident in table 27, the accumulated fluence metric produces a more accurate value - compared to the fluence per pulse value - which may be used to predict the color engraved on the stainless-steel sample. However, the average color difference value is still over 8 times the JND (where ΔE = 1). With that being said, perhaps another metric may be used in combination with the accumulated fluence in order to further narrow down which color will be produced.

	ΔE_{min}	ΔE_{avg}	ΔE_{max}
Fluence per Pulse	1.42	2.33	4.43
Accumulated Fluence	0.0	4.24	9.47

Table 28: CIE94 color difference values between colors engraved on hybrid card samples with the same fluence

The results for the hybrid card sample shown in table 28 are more accurate than the results for the stainless-steel samples in both methods. The average color difference values for the fluence per pulse and accumulated fluence calculations are almost one fifth and one half of the average values for the stainless-steel samples, respectively. These results seem more promising in terms of finding a single metric to predict the engraved color; although, they beg the question as to why there is such a large difference between sample types.

One potential explanation could be due to the size of the samples. Since the hybrid card samples were smaller than those which were only stainless steel, the cells within the test matrices were made to be smaller. In fact, they were just slightly larger than the spectrophotometer aperture. If the color is not consistent within the spectrophotometer aperture, it will take an average of all of the colors. If the cells engraved on the hybrid samples were too small to fully cover the aperture, it is likely that most of the CIEL*a*b* values collected are an average between the color of the test patch and the color of the unaltered sample. Therefore, the minimal color difference between cells on the hybrid card makes sense as each color was diluted by the background color of the card.

For some samples - such as those which have writing, line, or resolution tests - no negative impacts were seen by using the ultrasonic bath (although there was a slight color change). As for the color test samples, the process of cleaning the samples in the ultrasonic bath rendered the colors in the color matrices more inconsistent. Additional tests should be carried out with the samples staying in the ultrasonic bath for an increased amount of time to see if the inconsistencies are due to the material not being left in the bath long enough to be fully cleaned.

In the future it would be interesting to carry out similar experiments using a laser that has the capability to produce a higher pulse frequency because these types of parameters are typically required to produce more vibrant colors on metal.

5.2.   Comparison and Recommendations

In order to preserve the colors produced by the laser metal interactions, it is recommended that the metal be cleaned before engraving, post-engraving cleaning is avoided, and a protective coating is deposited on the metal surface after engraving.

Particularly in the case of payment card applications, material warping is not at all favorable. This could lead to a faulty card which cannot be inserted or swiped at a payment terminal. To avoid warping of the stainless steel or effecting the other materials of a hybrid card, air cooling should be introduced into the laser engraver for high fluence and slow speed engravings. If air cooling is not available, it is recommended to avoid the combinations of parameters displayed in tables 16 and 17.

Throughout these trials, it became evident that in order to generate color on the surface of the metal that was due to an oxidation layer, the laser must be set to low speeds, high power, and high pulse frequency. The speeds that were observed to produce color were those less than 200 mm/s. Primarily, around 160 mm/s, oxidation appeared to occur at powers greater than 70%. Due to the limitations of the F1 Ultra laser, 60 kHz was the highest frequency tested - and the only one that truly created color on the metal surface through marking.

As for engraving, a wide range of laser parameters proved to be sufficient to make engravings distinguishable from the background. Powers from 30 to 100% with speeds ranging from 1000 to 3000 mm/s allowed for the observation of whites, grays, and browns - which appeared matte.

Bibliography

[1] Linggamm, R., Quazi, M. M., Bashir, M. N., Aiman, M. H., Qaban, A., Dave, F., & Ali, M. M. (2021). A review on the formation of colors on SS304 stainless steel induced by laser color marking technique. *Journal of Advances in Technology and Engineering Research, 7*(2), 1–26. https://doi.org/10.20474/jater-7.2.1

[2] Kúdela, J., Andrejko, M., & Kubovský, I. (2023). The effect of CO_2 laser engraving on the surface structure and properties of spruce wood. Coatings, 13(2006). https://doi.org/10.3390/coatings13122006

[3] Kúdela, J., Kubovský, I., & Andrejko, M. (2022). Influence of irradiation parameters on structure and properties of oak wood surface engraved with a CO_2 laser. Materials, 15(8384). https://doi.org/10.3390/ma15238384

[4] Kamboj, A. (2024, September 11). Pyrolysis | Basic principles, types and uses. Engineeringa2z. Retrieved August 20, 2025, from https://www.engineeringa2z.com/pyrolysis-basic-principles-types-and-uses/

[5] Chernykh, M., Zykova, M., Stollmann, V., & Gilfanov, M. (2022). Influence effect of wood laser engraving mode on aesthetic perception of images. Acta Facultatis Xylologiae Zvolen, 64(2), 87–96. https://doi.org/10.17423/afx.2022.64.2.09

[6] Amara, E. H., Haïd, F., & Noukaz, A. (2015). Experimental investigations on fiber laser color marking of steels. Applied Surface Science, 351, 1–12. https://doi.org/10.1016/j.apsusc.2015.05.095

[7] Antonczak, A. J., Kocoń, D., Nowak, M., Kozioł, P., & Abramski, K. M. (2013). Laser-induced colour marking—Sensitivity scaling for a stainless steel. Applied Surface Science, 264, 229–236. https://doi.org/10.1016/j.apsusc.2012.09.178

[8] Nikolidakis, E., Karmiris-Obratanski, P., Papazoglou, E.-L., Karkalos, N. E., Markopoulos, P. A., & Antoniadis, A. (2023). Surface topography investigation during nanosecond pulsed laser engraving of SAE304 stainless steel. Materials Research Proceedings, 28, 1703–1710. https://doi.org/10.21741/9781644902479-184

[9] Veiko, V., Odintsova, G., Ageev, E., Karlagina, Y., Loginov, A., Skuratova, A., & Gorbunova, E. (2014). Controlled oxide films formation by nanosecond

laser pulses for color marking. Optics Express, 22(20), 24342–24347.
https://doi.org/10.1364/OE.22.024342

[10] xTool. (2025). *Laser machine comparison*. xTool. Retrieved July 22, 2025, from https://www.xtool.com/pages/laser-machine-comparison

[11] Otto Künnecke GmbH. (2019). DPS Smart: Desktop processing system for card and passport personalization [PDF].
https://www.kuennecke.com/wp-content/uploads/2019/06/DPS_Smart.pdf

[12] xTool Support Center. (2023). *What is the difference between engrave, score, and cut?* xTool. Retrieved July 3, 2025,
from https://support.xtool.com/article/565

[13] X-Rite, Incorporated. (2023). *eXact user guide*. X-Rite. Retrieved July 29, 2025,
from https://www.xritephoto.com/documents/Manuals/en/eXact_User_guide_en.pdf

[14] Nikon Instruments Inc. (2025). *SMZ1270 / SMZ1270i | Specifications*. Nikon Healthcare. Retrieved July 17, 2025,
from https://www.microscope.healthcare.nikon.com/products/stereomicroscopes-macroscopes/smz1270-smz1270i/specifications

[15] Kudzin, M. H., Piwowarska, D., Festinger, N., & Chruściel, J. J. (2024). Risks associated with the presence of polyvinyl chloride in the environment and methods for its disposal and utilization. *Materials, 17*(1), Article 173. https://doi.org/10.3390/ma17010173

[16] Adams, D. P., Hodges, V. C., Hirschfeld, D. A., Rodriguez, M. A., McDonald, J. P., & Kotula, P. G. (2013). Nanosecond pulsed laser irradiation of stainless steel 304L: Oxide growth and effects on underlying metal. *Surface and Coatings Technology, 222*, 1–8. https://doi.org/10.1016/j.surfcoat.2012.12.044

[17] ViewSonic Editorial Team. (2021). *What is Delta E? And why is it important for color accuracy?* ViewSonic. Retrieved July 2025,
from https://www.viewsonic.com/library/creative-work/what-is-delta-e-and-why-is-it-important-for-color-accuracy/

[18] Techkon USA. (2022). *A simple review of CIE ΔE* (color difference) equations*. Techkon. Retrieved August 2025,
from https://techkonusa.com/a-simple-review-of-cie-de-color-difference-equations

[19] ColorMine. (n.d.). CIE94 Delta E calculator. Retrieved August 21, 2025, from https://colormine.org/delta-e-calculator/cie94

Personal Statement of Non-Plagiarism

I hereby declare that all information in this report has been obtained and presented in accordance with academic rules and ethical conduct and the work I am submitting in this report, except where I have indicated, is my own work.
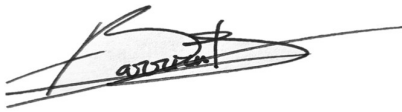
I acknowledge the use of Microsoft 365 Copilot [copilot.microsoft.com] to generate and debug code that was used to process the data presented in this report.

Supervisor's Approval

I, the undersigned, Jessica Pellegrino, supervisor of Teagan Kilian, student of the iPSRS EMJM, during her master thesis at Toppan Security certify that I approve the content of this master thesis report entitled "Laser Engraving on Stainless-Steel and Maple Wood as a Means of Customizing Payment Cards."

22/08/2025

Jessica Pellegrino